Processes controlling enrichment of transition elements in the surficial sediments of the western Bay of Bengal

C. Prakash Babu* and V. Ramaswamy

Geological Oceanography Division,
CSIR-National Institute of Oceanography, Dona Paula,
Goa 403 004, India

The processes leading to surficial enrichment of transition elements have been studied in continental slope and deep-sea sediments from the western Bay of Bengal (~500–4500 m water depth). The lower continental slope and rise (1800–3000 m) sediments are characterized by enrichment of Mn/Al ratios by 2–3 orders of magnitude and transition elements (Fe, Ni, Co, Cr and V) by a factor of 2–3 compared to the upper continental slope (500–1100 m) sediments. The occurrence of micronodules rich in Fe and Mn and elements associated with Mn–oxides, confirmed by scanning electron microscope and electron probe micro analysis, are responsible for the accumulation of transition elements in the lower continental slope sediments. The freshwater stratification, low carbonate productivity, fine grain size, low porosity, thin oxidized surficial layer and high sedimentation are conducive for diagenetic enrichment of Fe, Mn and elements associated with Mn–oxides in the lower slope sediments. The mid-depth oxygen minimum zone, resuspension and absence of oxidized surface layer enhance metal release to water column in the upper slope sediments. The oceanographic settings and high sedimentation rates control metal cycling in the Bay of Bengal sediments.

Keywords: Diagenesis, Fe–Mn micronodules, oxygen minimum zone, sedimentation, transition elements.

IN marine sediments, the transition elements like Fe, Mn, Cu, Ni, Co and Zn are concentrated during oxic and suboxic diagenetic processes[1,2]. Oxic diagenesis occurs at or near the sediment surface in slowly accumulating pelagic deep-sea sediments. This process involves release of Mn and other metals during decomposition of organic matter and dissolution of labile biogenic component to pore waters which are ultimately incorporated into sediments during early diagenesis[3,4]. The pore waters are characterized by the presence of dissolved oxygen and extremely low Mn concentration and diffusive flux to the overlying water column[2]. The occurrence of Mn nodules in slowly accumulating pelagic sediments is an example under this category[5–8]. On the other hand, regions experiencing high biological productivity and sedimentation suboxic diagenesis dominate. Thin oxidized surface layer overlie reducing sedimentary column in these regions[9]. The pore waters are low in dissolved oxygen, high dissolved Mn

concentration and diffusive flux towards the interface where dissolved Mn(II) is reoxidized to Mn(IV). The diagenetic enrichment of transition elements depends on the rate of organic carbon accumulation and degradation[10–12].

In the Bay of Bengal (BoB), accumulation of hydrolysable organic compounds is high due to enhanced sedimentation, organic mineral interaction and fine grain size[13–17], despite low productivity. The foraminifera carbonate productivity is low due to low salinity and freshwater stratification which inhibits mixing of nutrient-rich deep water with surface waters[18–20]. The mid-waters between 150 and 500 m are characterized by the presence of oxygen minimum zone (OMZ) (Figure 1 *a*)[21]. The main aim of the present study is to understand the spatial variations, enrichment and cycling of transition elements to decipher elemental mobilization and immobilization mechanisms in high-sedimentation BoB sediments.

Near-surface sediments from a wide depth range (480–4300 m) collected by gravity, spade and pilot piston cores during *ORV Sagar Kanya* cruises 157 and 187 from western BoB (Figure 1 *b* and Table 1) were chosen for this study. After sub-sampling the sediments were kept under cold conditions onboard and maintained at around 4°C temperature onshore in a cold room until further studies. Representative portions of the sediment samples were dried in a hot-air oven at 60°C, powdered to fine size and homogenized using an agate ball mill. The powdered samples were digested with HF, $HClO_4$ and HNO_3, the residue dissolved in 10 ml 6 N HCl and finally made to volume with distilled water. The digested solutions were analysed for major and minor elements using Perkin Elmer OPTIMA 2000 DV ICP-OES (inductively coupled plasma optical emission spectrometry). The analytical accuracy with respect to international reference material SCO-1 for major and minor elements is ±3% and ±9% (except Co) respectively. Calcium carbonate was determined by gasometric method with 'Karbonat Bombe' after acidification of the samples with 1 N HCl (ref. 22). The analytical accuracy with respect to international reference materials, viz. SGR-1 and SBC-1 is ±1%. Total organic carbon (TOC) was analysed using an elemental analyser (Carlo Erba CNS) after removing the inorganic carbon with HCl. The analytical accuracy with respect to international reference material MAG-1 is ±10%. Table 1 presents the sampling position details and analytical results.

Mn/Al ratios are high in the lower continental slope sediments by 2–3 orders of magnitude compared to the upper continental slope and deep-sea sediments (3176 versus 50×10^{-4}) (Figures 2 and 3). The coarse fraction (>63 μm) of only the lower slope sediments showed occurrence of micronodules when observed under binocular microscope. The micronodules are of various shapes and sizes when observed under scanning electron
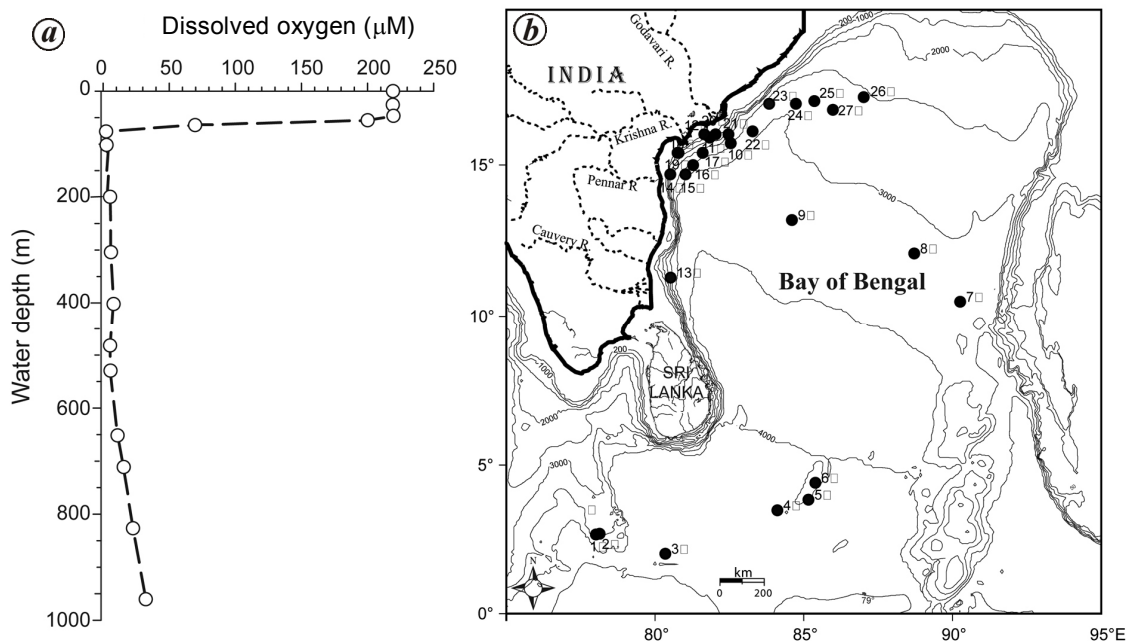
Figure 1. *a*, Vertical dissolved oxygen profiles at 19°N and 92°E in the Bay of Bengal (re-drawn after Naqvi[21]). *b*, Location map showing from where cores were retrieved. Depth contours are in metres.

Table 1. Sample position details, water depth (m) and transition element concentration

Station no.	Station id	Water depth (m)	Latitude (N)	Longitude (E)	Level (cm)	TOC	CaCO₃	Al	Fe	Mn	Cr	V	Co	Ni
								(wt %)				(ppm)		
1	SK 157/4[a]	3499	2.669	78.007	2–3	0.49	78.67	1.70	0.98	665	24	17	8	22
2	SK 157/5[d]	2972	2.669	78.006	0–1	0.49	75.24	1.09	0.62	369	17	11	5	13
3	SK 157/6[a]	4458	2.0189	80.341	0–1	0.55	49	4.27	2.54	986	59	53	18	50
4	SK 157/7[a]	4197	3.4851	84.111	2–3	0.47	50.75	3.54	1.91	1423	43	38	16	41
5	SK 157/9[a]	3568	3.8491	85.158	3–5	0.46	71.16	1.52	0.84	623	22	15	8	22
6	SK 157/12[a]	3439	4.4066	85.386	2–4	0.47	72.83	1.38	0.77	836	21	14	7	27
7	SK 157/17[a]	3220	10.516	90.255	1–3	0.56	46.08	3.77	1.94	1018	53	51	15	34
8	SK 157/20[a]	3202	12.147	88.711	4–5	0.49	46.41	3.78	2.06	1693	52	52	21	56
9	SK 157/23[a]	3260	13.227	84.603	0–1	1.06	23.43	6.26	3.99	2578	88	77	39	68
10	SK157/26[a]	2499	15.786	82.489	0–2	1.2	2.17	5.13	5.68	698	114	154	41	54
11	SK157/28[a]	1022	15.913	81.832	2–5	1.09	3.25	7.58	5.84	575	116	173	43	52
12	SK 157/29[a]	620	16.03	81.665	0–3	1.03	3.92	5.87	5.34	688	97	134	37	43
13	SK 187/9[c]	1950	11.316	80.52	0–1	1.52	4.83	5.22	3.90	259	96	93	24	47
14	SK 187/17[c]	1852	14.681	80.508	2–4	1.33	2.47	7.21	5.32	590	106	137	37	53
15	SK 187/18[a]	2777	14.736	81.023	0–2	1.52	3.33	5.62	5.36	548	104	141	37	50
16	SK 187/19[c]	2686	14.982	81.275	0–2	0.92	3.17	5.08	5.68	1129	106	169	45	48
17	SK 187/20[a]	2355	15.363	81.602	2–5	1.15	3.08	7.61	6.54	780	125	167	44	57
18	SK 187/21[b]	483	15.381	80.753	0–2	1.2	4.33	7.76	6.62	767	126	159	44	54
19	SK 187/21[a]	926	15.351	80.794	0–5	0.98	4.24	6.92	6.21	772	119	167	46	54
20	SK 187/23[a]	959	16.42	82.035	0–2	2.14	2.67	7.93	6.40	544	118	164	41	51
21	SK 187/24[c]	1945	16.039	82.474	0–2	1.14	2.12	4.28	5.19	812	100	147	38	46
22	SK 187/25[c]	2868	16.082	83.283	0–2	1.59	0.47	5.51	5.52	773	109	137	36	59
23	SK 187/27[c]	2645	17.03	83.741	2–4	1.25	0.25	6.49	5.37	5944	105	113	33	53
24	SK 187/28[c]	2829	17.022	84.47	1–3	1.4	0.7	5.83	5.03	12390	113	122	34	57
25	SK 187/29[c]	2710	17.063	85.15	0–2	1.24	0.61	4.88	4.67	15500	105	113	34	57
26	SK 187/30[a]	2579	17.093	86.752	0–5	1.26	6.75	5.88	4.75	6250	107	100	28	55
27	SK 187/33[c]	3003	16.265	84.5	0–2	1.48	0.73	4.89	4.11	1131	101	116	28	50
	SCO-I (reported)							7.25	3.59	410	68	130	11	27
	Obtained (*n* = 4)							7.05	3.65	404	74	129	17	25
	Ganges[37]							4.60	2.10	400	52	86	22	20
	Brahmaputra[37]							5.60	2.90	644	100	137	31	47
	KG Basin[33]							8.04	6.35	800	129	192	30	84

[a]Gravity core; [b]Piston core; [c]Piston (pilot) core; [d]Spade core.
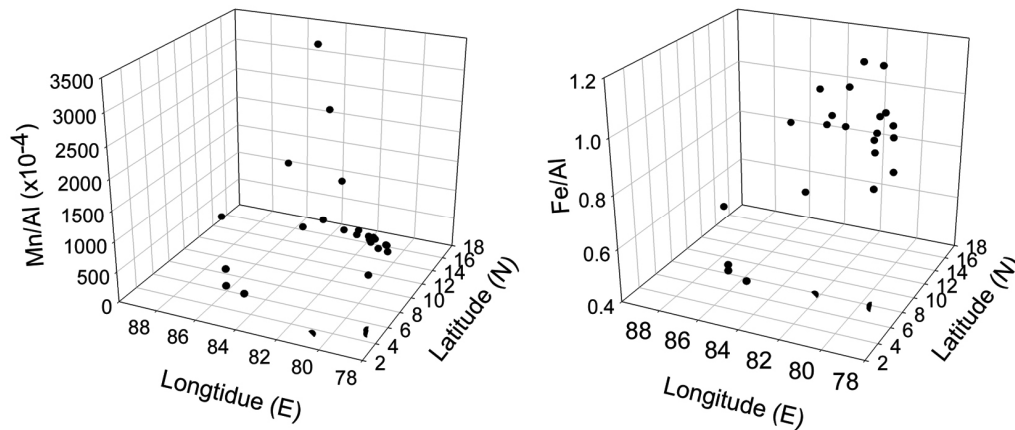
Figure 2. The diagenetic enrichment of Mn and Fe in northern Bay of Bengal sediments.
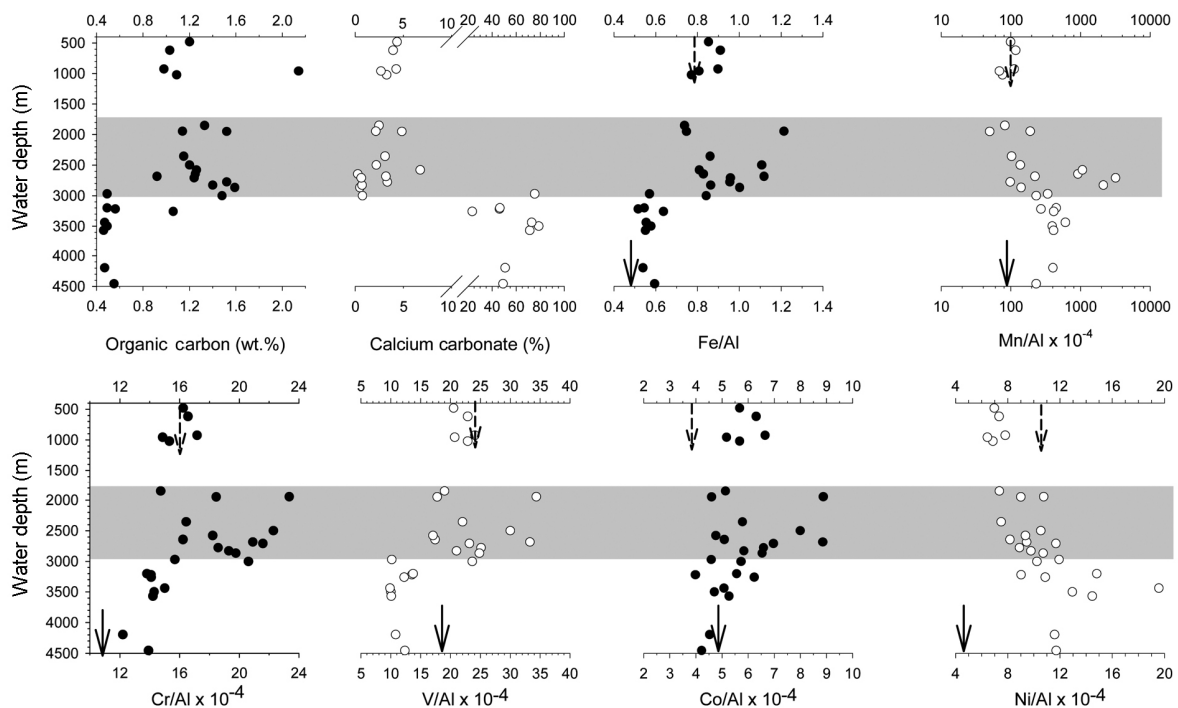

Figure 3. Water depth versus metal/Al ratio of transition metals. The shaded region shows enrichment of transition elements at greater depths of continental slope sediments. The solid and dashed arrows denote the average metal/Al values of the Ganges[37] and KG basin sediments[33]. Note log scale for Mn/Al ratios.

microscope (SEM) (Figure 4 a–c). The micronodules are rich in Fe and Mn and other transition elements associated with Mn-oxides when analysed using energy dispersive spectrum (EDS) and electron probe micro analyser (EPMA) (Tables 2 and 3). The occurrence of Fe–Mn micronodules is the main reason for Mn enrichment and high Mn/Al ratios in the lower slope sediments. Fe–Mn micronodules were reported earlier at greater depths in the middle Bengal Fan due to high sedimentation[23–25]. Mn is supplied mainly through hydrogenetic sources, aeolian, hydrothermal, glacial and early diagenesis[7,26–28]. In the present study, the supply of Mn from hydrogenetic source

is ruled out as this source dominates in open ocean sediments least influenced by terrigenous material. There are no reports of either glacial or hydrothermal activity in the study area, ruling out Mn contribution from these sources. Dust activity does not contribute significant Mn to the BoB sediments. Repeated cycling of Mn mobilization and immobilization under thin oxic layer due to high sedimentation during early diagenesis can explain high Mn/Al ratios in the present study.

The oxidants, viz. dissolved oxygen, nitrate, Mn oxides, Fe_2O_3 and sulphate are utilized in sequence for organic matter oxidation in the continental margin sediments[29,30].
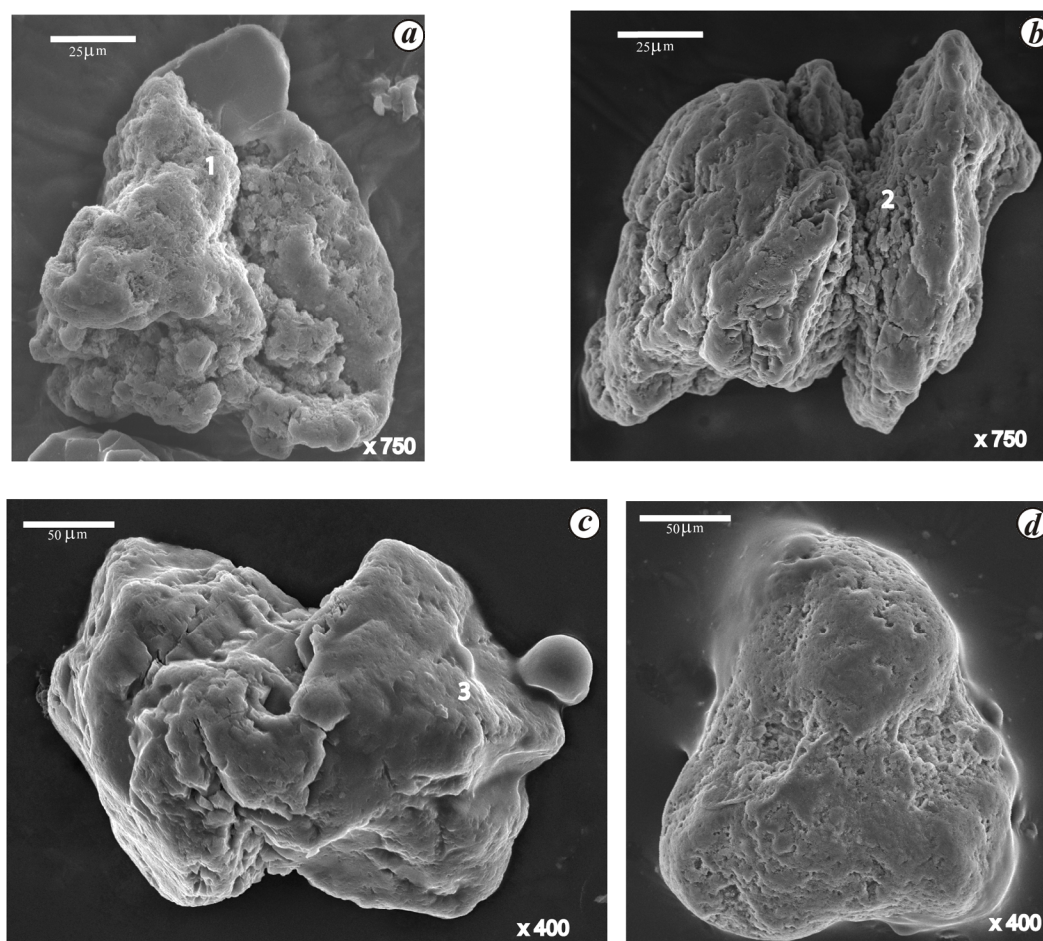
Figure 4. Scanning electron microscope images of Mn micronodules: *a*, botroidal; *b*, cemented; *c*, smooth; *d*, botroidal with dissolution pits from SK 187/GC 30 samples. The numbers indicate EDS spot analysis.

Table 2. Energy dispersive spectrum microprobe spot analysis of micronodules (wt%) in a sediment sample (SK 187/GC 30)

Spot no.	Si	Al	Fe	Mn	Ca	K	Mg	Cu	Zn	Mn/Fe
1	6.69	2.30	1.31	49.89	2.40	0.74	4.26	1.12	1.90	38.1
2	4.39	1.30	1.65	56.19	2.68	0.61	3.04	1.09	1.90	34.1
3	1.24	0.34	5.47	62.46	1.51	0.50	0.26	1.59	2.47	11.4
Bay of Bengal[23]	–	1.74	1.46	25.21	1.33	–	–	0.65	0.14	17.3
Indian Ocean[7]	–	0.66	1.38	35.02	1.64	–	–	1.62	0.37	25.4

The dissolved oxygen is used rapidly within the top few millimeters in the sediment column due to quick burial of labile organic carbon. Sub-oxic conditions develop in the sedimentary column overlie by a thin oxidized surficial layer due to oxic water column[31]. In the absence of dissolved oxygen, the oxygen in MnO_2 is used as an alternate oxidant for organic matter degradation in the sub-oxic sediment column. A portion of the non-lithogenic fraction of Mn in the sediments is mobilized as dissolved Mn^{2+} and built-up to high concentrations in pore waters compared to the overlying water column. Mn is also removed from solid phase Mn-micronodules from the sedimentary column to pore waters[23]. The dissolved Mn released from the sedimentary column as well as micronodules built up in pore water, develops a concentration gradient, diffuses towards the interface and precipitate as MnO_2 under oxic bottom-water conditions. With further sedimentation and arrival of fresh organic matter, freshly precipitated Mn (oxy)hydroxides are buried again. With the development of sub-oxic conditions in the sediment column, MnO_2 is again used as an oxidant for organic matter oxidation. Thus, a continuous cycle of Mn-oxides burial, release, diffusion and immobilization enriches Mn concentration and micronodule formation.

Table 3. Spot analysis of a radiolarian test from a sediment sample (SK 187/GC 28) by electron probe micro analyser

|	Si	Al	Fe	Mn	Ca	K	Mg	Cu	Zn	Mn/Fe
Spot no.	(wt %)									
1.1	9.20	4.12	3.65	19.31	2.36	9.20	1.89	0.03	0.30	5.2
1.2	14.00	4.00	3.22	9.35	0.69	0.20	0.70	b.d.	0.11	2.9
1.3	9.88	1.00	0.10	9.22	0.78	0.09	0.42	b.d.	0.14	92.2
1.4	9.60	0.76	0.12	4.25	0.44	0.08	0.19	b.d.	0.12	35.4
1.5	12.70	2.19	0.14	1.07	0.19	0.08	0.10	b.d.	0.03	7.6
1.6	5.90	1.05	0.32	7.16	0.62	0.08	0.44	0.02	0.15	22.4
1.7	14.10	2.16	0.93	13.39	1.08	0.30	0.93	0.01	0.33	14.4
1.8	17.70	2.18	0.81	10.16	0.89	0.25	0.60	0.07	0.28	12.5
1.9	12.30	1.39	0.45	15.54	1.28	0.20	0.71	0.03	0.26	34.5
1.10	5.20	1.93	1.25	29.81	2.13	0.40	1.81	b.d.	0.41	23.9
2.1	5.21	2.19	1.31	30.01	2.27	0.40	1.83	0.07	0.53	22.9
2.2	13.60	1.66	0.52	24.20	1.88	0.24	1.15	0.05	0.37	46.5
2.3	9.77	2.23	0.44	26.04	2.05	1.50	1.45	0.09	0.50	59.2
2.4	2.31	1.53	0.94	38.22	2.63	0.36	2.30	b.d.	0.38	40.7
2.5	8.73	2.07	1.91	29.43	2.39	0.28	1.66	0.02	0.56	15.4

b.d, Below detection.
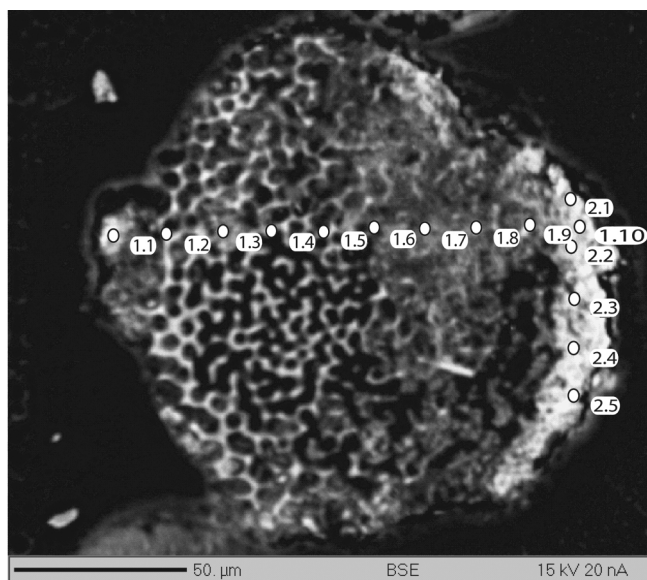
Figure 5. SEM image of a radiolarian test (SK 187/GC 28) showing Mn precipitation within a siliceous test. The numbers indicate spots where EPMA analysis was carried out.

The Mn diagenetic cycling is driven by the nature of labile organic carbon and decomposition rates. The high sedimentation enhances faster burial of labile organic carbon. Fine grain size and low porosity favour the development of reducing conditions in the sediment column close to the interface. The release of Mn from the sedimentary column, micronodules and precipitation as Mn(oxy)hydroxides due to oxygenated water column and thin oxic layer enrich Mn in the lower slope sediments in the present study. In the upper slope sediments, the development of reducing conditions either in the water column or close to the interface due to the presence of

mid-depth OMZ may prevent the formation of oxidized layer for Mn(oxy)hydroxide precipitation. The dissolution of oxyhydroxides in sediments due to low dissolved oxygen concentration in the water column has been reported earlier[32]. The dissolved Mn^{2+} accumulated in the pore water may diffuse to the overlying water column due to the absence of oxic conditions at the interface for precipitation. Alternatively, slumping/sliding of the upper slope sediments may resuspend the sediments, which limits metal accumulation. Mn spatial variations due to textural differences are ruled out as fine-sized silty clay sediments carpet the slope regions of the study area[33,34].

The micronodules separated from the coarse fraction (>63 μm) were examined under SEM (JOEL 5800 LV) for morphological features. Micronodules of different shapes and sizes (Figure 4 a–c) with dissolution pits (Figure 4 d) were observed (SK 187/GC 30). EDS analysis (Oxford) of these micronodules showed very high Mn (50–62%), Cu and Zn concentrations (1.00–2.50%) (Table 3) confirming diagenetic remobilization of Mn^{2+}, followed by its oxidation as MnO_2 and uptake of dissolved trace elements. Higher concentrations of Mn^{2+} and Mn-oxide associated elements in micronodules have been reported earlier from the BoB sediments in the study area[25]. The dissolution pits observed on the micronodules indicate precipitation of MnO_2 in the biological test, which retain the spheroidal shape after dissolution of the test (Figure 4 d). A radiolarian test (SK 187/GC 28) when analysed using EPMA (Cameca SX-5) confirmed gradual precipitation of Mn in the biological test (Figure 5 and Table 3). The enrichment of Mn (13–30%) and concomitant decrease in Si and Al concentrations towards the periphery of a radiolarian test indicate gradual dissolution of siliceous test. The micro probe analysis when focused on the periphery showed Mn enrichment up to 24–30%

(spot nos 2.1–2.5) (Figure 5 and Table 3). High Mn/Fe ratios obtained by EDS as well as EPMA reveal Mn enrichment during early diagenesis.

Along with Mn, the transition metal/Al ratios of Fe, Co, Cr and V (except Ni/Al) are also high by a factor of 2–3 in the lower continental slope compared to the upper slope and deep sea sediments (Figure 3). During sub-oxic diagenesis along Mn other transition elements (Cu, Ni, Co and Zn) are also released to the pore waters. These transition elements diffuse through pore waters towards the interface and sorbed on to Fe–Mn(oxy)hydroxides[35,36]. Thus along with Mn elements associated with Fe–Mn(oxy)hydroxides are also enriched in the lower slope surface sediments (Figure 3).

An evidence for the development of reducing conditions close to the interface is provided by the accumulation of biogenic elements (Cr and V; Figure 3). Faster burial of organic matter which limits oxygen exposure time for degradation and development of reducing conditions close to the interface seem to enhance preservation of biogenic elements. Several major rivers, viz. the Ganges, Brahmaputra, Godavari, Krishna, Cauvery and Mahanadi debouch huge quantities of fine-sized fluvial and clastic sediments to BoB. The organic matter is removed from the water column rapidly by settling lithogenic material (ballast effect) which enhances the preservation of hydrolysable organic compounds in surface sediments from BoB[13–17]. Factors other than sedimentation also contribute to the development of reducing conditions close to the interface. The fine-sized sediments, low porosity, gentle gradient, less foraminifera carbonate productivity[20,25,33,34] and thin oxidized surface layer limit diffusion of nutrients between pore waters and bottom waters, leading to the development of reducing conditions close to the interface and preservation of biogenic elements.

1. Hong, J., Calmano, W. and Förstner, U., Interstitial waters. In *Trace Elements in Natural Waters* (eds Salbu, B. and Steinnes, E.), CRC Press, Boca Raton, 1995, pp. 117–150.
2. Shaw, T. J., Gieskes, J. M. and Jahnke, R. A., Early diagenesis in differing depositional environments: the response of transition metals in pore water. *Geochim. Cosmochim. Acta*, 1990, **54**, 1233–1246.
3. Burdige, D. J., The biogeochemistry of manganese and iron reduction in marine sediment. *Earth Sci. Rev.*, 1993, **35**, 249–284.
4. Sundby, B. and Silverberg, N., Manganese fluxes in the benthic boundary layer. *Limnol. Oceanogr.*, 1985, **30**, 374–382.
5. Stoffers, P., Glasby, G. P., Thijssen, T., Shrivastva, P. and Melguen, M., The geochemistry of coexisting manganese nodules, micronodules, sediments and pore waters from five areas in the equatorial and Southwest Pacific. *Chem. Erde*, 1981, **40**, 273–297.
6. Kunzendorf, H., Glasby, G. P., Stoffers, P. and Renner, R. M., The distribution of rare earth elements in manganese nodules, micronodules and sediments along an east–west transect in the Southern Pacific. *Lithos*, 1989, **30**, 45–56.
7. Pattan, J. N., Manganese micronodules: a possible indicator of sedimentary environments. *Mar. Geol.*, 1993, **113**, 331–344.
8. Pattan, J. N., Colley, S. and Higgs, N. C., Behavior of rare earth elements in coexisting manganese macronodules, micronodules and sediments from the central Indian Basin. *Mar. Georesour. Geotechnol.*, 1994, **12**, 283–295.
9. Lyle, M., The brown–green color transition in marine sediments: a marker of the Fe(III)–Fe(II) redox boundary. *Limonol. Oceanogr.*, 1992, **28**, 1026–1033.
10. Brumsack, H.-J., Geochemistry of recent TOC-rich sediments from The Gulf of California and the Black Sea. *Geol. Rundsch.*, 1989, **78**, 851–882.
11. Brumsack, H.-J., The trace metal content of recent organic carbon rich sediments: implications for Cretaceous black shale formation. *Palaeogeogr., Palaeoclimatol., Palaeoecol.*, 2006, **232**, 344–361.
12. Calvert, S. E. and Pedersen, T. F., Geochemistry of recent oxic and anoxic marine sediments: implications for the geological record. *Mar. Geol.*, 1993, **113**, 67–88.
13. Bhosle, N. B. and Dhople, V. M., Distribution of some biochemical compounds in the sediments of the Bay of Bengal. *Chem. Geol.*, 1988, **67**, 341–352.
14. Ittekot, V., The abiotically driven biological pump in the ocean and short term fluctuations in the atmospheric CO_2 contents. *Global Planet. Change*, 1993, **8**, 17–25.
15. Subramanian, V., Sediment load of Indian rivers. *Curr. Sci.*, 1993, **64**, 928–930.
16. Ramaswamy, V. and Nair, R. R., Fluxes of material in the Arabian Sea and Bay of Bengal-sediment trap studies. *Proc. Indian Acad. Sci. (Earth Planet. Sci.)*, 1994, **103**, 189–210.
17. Unger, D., Ittekot, V., Schäfer, P. and Tiemann, J., Biogeochemistry of particulate organic matter from the Bay of Bengal as discernible from hydrolysable neutral carbohydrates and amino acids. *Mar. Chem.*, 2005, **96**, 155–184.
18. Prasad, T. G., Annual and seasonal mean buoyancy fluxes for the tropical Indian Ocean. *Curr. Sci.*, 1997, **73**, 667–674.
19. Prasanna Kumar, S. *et al.*, Why is the Bay of Bengal less productive during summer monsoon compared to the Arabian Sea? *Geophys. Res. Lett.*, 2002, **29**(24), 88.1–88.4.
20. Ramaswamy, V. and Gaye, B., Regional variations in the fluxes of foraminifera carbonate, coccolithophorid carbonate and biogenic opal in the northern Indian Ocean. *Deep-Sea Res. I*, 2006, **53**, 271–293.
21. Naqvi, S. W. A., Oxygen deficiency in the northern Indian Ocean. *Suppl. Gayana*, 2006, **70**, 53–58.
22. Müller, C. and Gastner, M., The 'Karbonat Bombe' a simple device for the determination of the carbonate content in sediments, soils and other materials. *Neu. Jb. Mineral. Mh.*, 1971, **10**, 466–469.
23. Chauhan, O. S., Gujar, A. R. and Rao, Ch. M., On the occurrence of ferromanganese micronodules from the sediments of the Bengal Fan: a high terrigenous site. *Earth Planet. Sci. Lett.*, 1994, **128**, 563–573.
24. Chauhan, O. S. and Rao, Ch. M., Influence of sedimentation on enrichment of manganese and growth of ferromanganese micronodules, Bengal Fan, India. *Mar. Geol.*, 1999, **161**, 39–47.
25. Chauhan, O. S., Geochemistry of ferromanganese micronodules and associated Mn and trace metals diagenesis at high terrigenous depositional site of middle fan region, Bay of Bengal. *Deep-Sea Res. II*, 2003, **50**, 961–978.
26. Klinkhammer, G., Heggie, D. T. and Graham, D. W., Metal diagenesis in oxic marine sediments. *Earth Planet. Sci. Lett.*, 1982, **61**, 211–219.
27. Dymond, J., Lyle, M., Finney, B., Piper, D. Z., Murphy, K., Conrad, R. and Pisias, N., Ferromanganese nodules from MANOP sites H, S, and R: control of mineralogical and chemical composition by multiple accretionary processes. *Geochim. Cosmochim. Acta*, 1984, **48**, 93l–949.

28. Stoffers, P., Glasby, G. P. and Frenzel, G., Comparison of the characteristics of manganese micronodules from the equatorial and southwest Pacific. *Tscher. Miner. Petrog.*, 1984, **33**, 1–23.

29. Froelich, P. N. *et al.*, Early oxidation of organic matter in pelagic sediments of the eastern and equatorial Atlantic: sub-oxic diagenesis. *Geochim. Cosmochim. Acta*, 1979, **43**, 1075–1090.

30. Postma, D. and Jakobsen, R., Redox zonation: equilibrium constrains on the Fe(III)/SO$_4$-reduction interface. *Geochim. Cosmochim. Acta*, 1996, **60**, 3169–3175.

31. Lynn, D. C. and Bonatti, E., Mobility of manganese in diagenesis of deep sea sediments. *Mar. Geol.*, 1965, **3**, 457–474.

32. Chakraborty, P., Chakraborty, S., Jayachandran, S., Madan, R., Sarkar, A., Linsy, P. and Nagender Nath, B., Effects of bottom water dissolved oxygen variability on copper and lead fractionation in the sediments across the oxygen minimum zone, western continental margin of India. *Sci. Total Environ.*, 2016, **556**, 1052–1061.

33. Pattan, J. N., Parthiban, G., Prakash Babu, C., Khadge, N. H., Paropkari, A. L. and Kodagali, V. N., A note on geochemistry of surface sediments from Krishna–Godavari basin, east coast of India. *J. Geol. Soc. India*, 2008, **71**, 107–114.

34. Prakash Babu, C. and Ramaswamy, V., Phosphorus accumulation associated with intense diagenetic metal-oxide cycling in sediments along the eastern continental margin of India. *Curr. Sci.*, 2017, **113**(3), 473–478.

35. Burns, R. G. and Burns, V. M., Authigenic oxides. In *The Sea, Volume 7, The Oceanic Lithosphere* (ed. Emiliani, C.), Wiley-Interscience, New York, USA, 1981, pp. 875–914.

36. Balistrieri, L. S. and Murray, J. W., The surface chemistry of sediments from the Panama Basin: the influence of Mn oxides on metal adsorption. *Geochim. Cosmochim. Acta*, 1986, **50**, 2235–2243.

37. Subramanian, V., 'T Dack, L. V. and Grieken, R. V., Chemical composition of river sediments from the Indian sub-continent. *Chem. Geol.*, 1985, **48**, 271–279.

Estimation of rock load in development workings of underground coal mines – a modified RMR approach

Avinash Paul[1,*], Vemavarapu Mallika Sita Ramachandra Murthy[2], Amar Prakash[1] and Ajoy Kumar Singh[1]

[1]Central Institute of Mining and Fuel Research, Dhanbad 826 015, India
[2]Department of Mining Engineering, Indian Institute of Technology (Indian School of Mines), Dhanbad 826 004, India

Underground coal mining in India contributes to a share of 55 Mt production with more than 500 mines in operation. In spite of using the well-established CMRI-ISM Rock Mass Rating (RMR$_{dyn}$) classification system for roof support design successfully in Indian geo-mining conditions, accidents due to roof fall constitute the major challenge. These failures are generally due to the presence of weak beddings and laminations. Seismic refraction technique (for shallow depth) can be useful in detecting the rock mass conditions. Based on the study a modified rock mass classification system (RMR$_{dyn}$) was setup by incorporating field *P*-wave velocity with a view to arrive at a real ground condition of the *in situ* rock. Rock loads were also determined in the field to develop a relation with RMR$_{dyn}$. A comparison of rock load estimation by CMRI-ISM RMR, numerical simulation and RMR$_{dyn}$ clearly depicts that the latter approach is more reliable as the results are close to the actual scenario.

Keywords: CMRI-ISM RMR, RMR$_{dyn}$, *P*-wave velocity, rock load, support design.

ROCK mass classification systems have constituted an integral part of empirical mine design for over 100 years[1]. An important contribution of the rock mass rating (RMR) is that the system has stimulated the development of a plethora of more specialized systems of ground evaluation, particularly in mining application[2]. It provides guidelines for stability assessment and also to select the appropriate support system[3].

Ground movement is a serious concern in underground coal mines[4]. Roof fall generally takes place due to detachment of lower strata since the redistribution of stresses takes place around the excavation made[5]. Blasting in the development faces is also one of the major causes of roof damage due to lack of free face and consequent higher order ground vibrations[6]. The strength of roof rock can be improved by installing timely supports with adequate capacity[7,8]. Thus, proper rock load assessment and support design for mine openings are considered as major factors in the stability of the roof strata[9,10].

*For correspondence. (e-mail: avinashpaul02@yahoo.co.in)